CHAPTER IV

RESULTS AND DISCUSSION

1. The Study of High-Performance Liquid Chromatographic Conditions

The separation of 16 PAHs i.e., Naph, Acenl, Acent, Flu, Phen, Ant, Flt, Pyr, BaA, Chry, BbF, BkF, BaP, Dah, Bghi, and Ind was studied by two types of the analytical columns : Nova-Pak C_{18} (monomeric type) and Vydac C_{18} (polymeric type). For the Nova-Pak C_{18} column, Acent, Flu, BaA, Chry, BbF, BkF, Bghi, and Ind were only partially resolved. Moreover, the analysis time was very long (35 min). However, on the Vydac C_{18} column, separation of all 16 PAHs was achieved with only 22 min of the analysis time. Therefore, Vydac C_{18} column was considered to be chosen to analyse these 16 PAHs. The optimum HPLC conditions for separation of 16 PAHs were summarised in Table 4.1.

The maximum wavelengths of each PAHs were shown in Table 4.2. Because the maximum wavelengths of each PAHs were vary, the analysis at maximum wavelength was complicated. The optimum wavelengths of each PAHs were chosen for this study to compromise the complication of analysis and sensitivity of each PAHs. The chromatograms of 1.00 ppm standard mixture of 16 PAHs at 230, 270, and 350 nm were shown in Figures 4.1-A, 4.1-B, and 4.1-C respectively.

The most compound had high sensitivity at 270 nm except Acent and Acenl had high sensitivity at 230 nm. The sensitivity of Ant at 230 nm was higher than at 270 nm. So that, the optimum wavelength of Acent, Acenl, and Ant were 230 nm. Figure 4.1-A had the ghost peaks at retention time 5.422 min and 14.222 min and peak of BaP at retention time 15.772 min was very broad. Figure 4.1-B had the ghost peaks at retention time 14.105 min and peak of BkF at retention time 15.105 min had tailing. So that, BbF, BkF, BaP, Dah, Bghi, and Ind were not suitable to analyse at 230 and 270

nm. They were analysed at 350 nm to avoid the interference of the ghost peaks. The optimum wavelengths used to quantify each PAHs were shown in Table 4.2

Table 4.1 The optimum HPLC conditions

Parameter	Condition
Column	
Analytical Column	Vydac C_{18} column 250 x 4.6 mm I.D., 5 μm
Guard Column	Vydac C_{18} guard column 30 x 2 mm I.D., 5 μm
Mobile Phase	Isocratic elution for 2 min by using acetonitrile-water (60:40, v/v); then linear gradient to 100% acetonitrile in 6 min; pure acetonitrile for 12 min and linear gradient once again to acetonitrile-water (60:40, v/v) in 2 min
Equilibration Time	15 min
Flow Rate	1.5 mL/min
Injection Volume	10 μL
Detector	Photodiode Array Detector
Data Acquisition Parameters	
Start Wavelength	200 nm
End Wavelength	400 nm
Rate	1.0 spec/sec
Resolution	4.8 nm

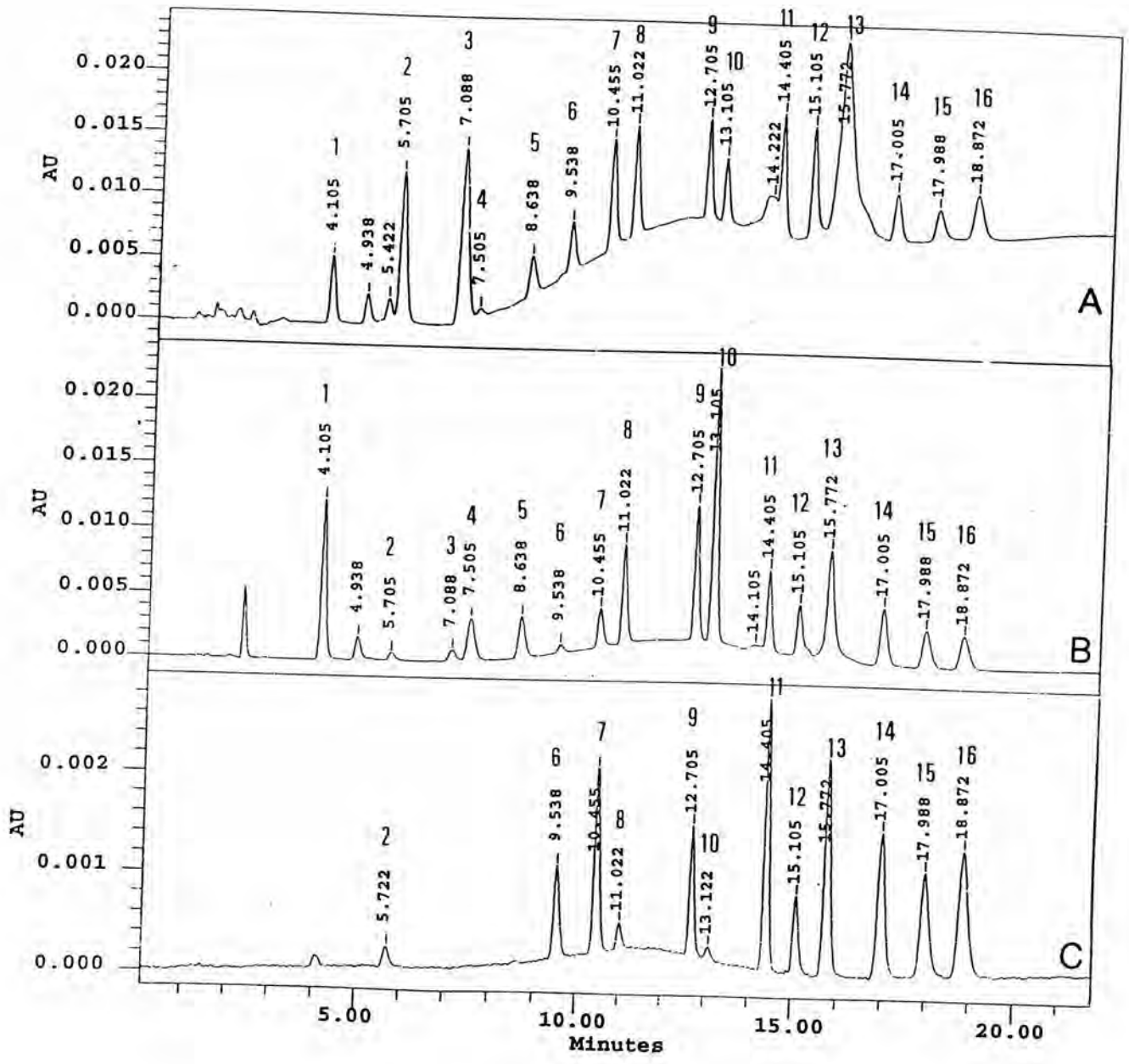

Figure 4.1 The chromatogram of 1.00 ppm standard mixture of 16 PAHs by HPLC conditions in Table 4.1. For peak assignment, see Table 4.2

A At 230 nm

B At 270 nm

C At 350 nm

Table 4.2 Abbreviation, maximum wavelength (λ_{max}), optimum wavelength used for measuring the absorbance (λ_{op}), and retention (t_R) of each PAHs

Compound			λ_{max} (nm)	λ_{op} (nm)	t_R
No.	Name	Abbreviation			
1	Naphthalene	Naph	220	270	4.938
2	Acenaphthylene	Acenl	230	230	5.705
3	Acenaphthene	Acent	230	230	7.088
4	Fluorene	Flu	210	270	7.505
5	Phenanthrene	Phen	252	270	8.638
6	Anthracene	Ant	252	230	9.538
7	Fluoranthene	Flt	210,235	270	10.455
8	Pyrene	Pyr	238	270	11.022
9	Benzo[a]anthracene	BaA	288	270	12.705
10	Chrysene	Chry	268	270	13.105
11	Benzo[b]fluoranthene	BbF	258	350	14.405
12	Benzo[k]fluoranthene	BkF	240	350	15.105
13	Benzo[a]pyrene	BaP	295	350	15.772
14	Dibenzo[a,h]anthracene	Dah	295	350	17.005
15	Benzo[g,h,i]perylene	Bghi	300	350	17.988
16	Indeno[1,2,3-cd]pyrene	Ind	248	350	18.872

2. The Creation of Spectral Library

The Spectral library was created from the chromatogram of 1.00 ppm standard solution of PAHs mixture. The spectra of each PAHs in the spectral library were shown in Figure 4.2.

The Millinium PDA software uses the Spectral Contrast technique for spectrum matching or library search. This technique quantifies differences in spectral shapes by converting spectra to vectors and comparing the vectors. The matching results are displayed in the Match Angle value. It is a measure of the difference in spectral shape between an unknown spectrum and a library spectrum. Valid Match Angle results are between 0 to 90. A value of 0 indicates a perfect match. In this study, the Match Angle value of 20 was conceded.

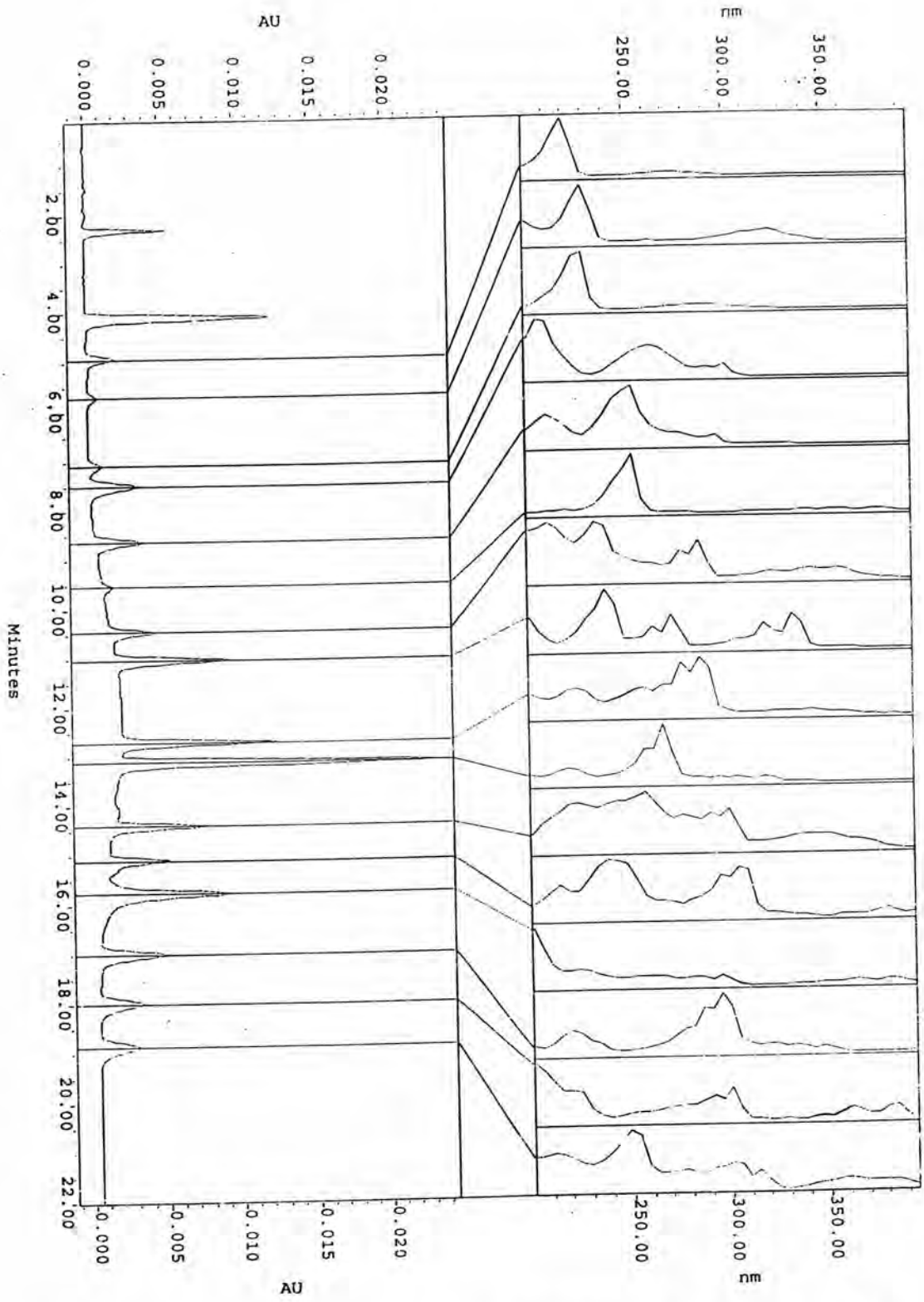

Figure 4.2 The spectrum and chromatogram of 16 PAHs in the spectral library by HPLC conditions in Table 4.1. For peak assignment, see Table 4.2

3. The Study of Linearity of Standard PAHs

Linearity of the response for each PAHs was performed in the range of 0.1-100 ppm. The plots of relationship between concentration of each PAHs and peak area were shown in Appendix B. Moreover, the linear regression data for linearity studies of all PAHs were shown in Table 4.3.

The linearities of each PAHs were shown in form of correlation coefficients (R). From Table 4.3, the correlation coefficients obtained were between 0.9936 and 0.9991. Thus, all curves were good linear. Because all curves did not depart from linearity, it could be said that all PAHs were good linearity though at 100.00 ppm. The compound that higher correlation coefficient was higher linearity. So that, Flt was highest linearity and Chry was lowest linearity in this study.

In addition, the sensitivities of each PAHs could indicated by slope. Similar to linearity, the compound that higher slope was higher sensitivity. Thus, Acent was highest sensitivity and BkF was lowest sensitivity in this study.

Table 4.3 Linear regression data for linearity of 16 PAHs

Compound	Intercept (10^5 μV·sec)	Slope (10^5 V·sec·cm^3·g^{-1})	R
Naph	0.1036	0.1755	0.9988
Acenl	1.0698	1.1492	0.9978
Acent	1.4747	1.2125	0.9964
Flu	0.1870	0.3891	0.9990
Phen	0.2025	0.3335	0.9989
Ant	0.3710	0.4042	0.9979
Flt	0.1647	0.2872	0.9991
Pyr	0.5350	0.6856	0.9985
BaA	0.5815	0.8121	0.9987
Chry	1.9956	1.1092	0.9936
BbF	0.1247	0.2061	0.9990
BkF	0.0363	0.0678	0.9990
BaP	0.1229	0.2065	0.9989
Dah	0.0916	0.1498	0.9989
Bghi	0.0766	0.1444	0.9991
Ind	0.1201	0.1950	0.9989

4. The Study of Calibration Curve of Standard PAHs

The calibration curves for all PAHs were studied over the range of 100-800 ppb. These curves were shown in Appendix B. Linear regression datas for calibration curve studies of 16 PAHs were shown in Table 4.4.

The linearities of each curves were shown in form of correlation coefficients (R). From Table 4.4, these curves were good linear with the correlation coefficient of 0.9901-0.9979. Like the study of linearity, the calibration curve of Naph was highest linearity and the calibration curve of Dah was lowest linearity. Moreover, Acent was highest sensitivity and BkF was lowest sensitivity in this study.

Table 4.4 Linear regression data for calibration curve of 16 PAHs

Compound	Intercept (10^2 μV·sec)	Slope (10^2 V·sec·cm^3·mg^{-1})	R
Naph	-0.3025	0.1600	0.9979
Acenl	3.9761	1.0772	0.9975
Acent	-0.6040	1.2171	0.9951
Flu	-0.6652	0.3455	0.9953
Phen	0.2763	0.3077	0.9932
Ant	1.6104	0.3614	0.9968
Flt	1.4716	0.2531	0.9928
Pyr	4.4633	0.5933	0.9932
BaA	3.6461	0.7168	0.9908
Chry	4.7179	1.1914	0.9907
BbF	0.6544	0.1876	0.9916
BkF	0.1058	0.0598	0.9923
BaP	0.7033	0.1810	0.9923
Dah	0.3452	0.1328	0.9901
Bghi	0.0850	0.1344	0.9928
Ind	0.3055	0.1782	0.9921

5. The Study of Detection Limit

The detection limit of the instrument was defined as the amount of analyte in standard solutions that yields a peak at signal-to-noise ratio equal to 3. The detection limits of each PAHs were shown in Table 4.5.

The high sensitivity compound would have low detection limit i.e. Pyr, BaA, and Chry. While, the lower sensitivity compound would have higher detection limit i.e. Naph, BbF, BkF, BaP, Dah, Bghi, and Ind. In contrast, Acenl, Acent, Flu, and Ant had high sensitivity but their detection limits were high because of the interference from ghost peaks and background. From Table 4.5, the sample solutions which the concentrations of 16 PAHs were less than 8 ppb could not analyse by these HPLC conditions. So that, the sample preparation was necessarily for preconcentration.

Table 4.5 The detection limits of 16 PAHs

Compound	Detection Limit (ppb)
Naphthalene	30
Acenaphthylene	25
Acenaphthene	30
Fluorene	60
Phenanthrene	30
Anthracene	60
Fluoranthene	15
Pyrene	8
Benzo[a]anthracene	8
Chrysene	8
Benzo[b]fluoranthene	30
Benzo[k]fluoranthene	30
Benzo[a]pyrene	30
Dibenzo[a,h]anthracene	30
Benzo[g,h,i]perylene	30
Indeno[1,2,3-cd]pyrene	30

6. The Study of Various Effects on the Percent Recovery of Small Disk Extraction Method

6.1 The Effect of The Concentration of 2-Propanol

The concentrations of 2-propanol were studied at 0, 5, 10, 15, and 20% 2-propanol in 2.00 ppb spiked standard solutions. The results of 2-propanol concentrations on the percent recoveries of each PAHs were presented in Table 4.6. The plot of relationship between the percent recoveries and each of PAHs for each of 2-propanol concentrations was shown in Figure 4.3.

The recoveries of 16 PAHs were between 26-98% when no adding 2-propanol. When adding 5% of 2-propanol, the recoveries of 15 PAHs i.e. Acenl, Acent, Flu, Phen, Ant, Flt, Pyr, BaA, Chry, BbF, BkF, BaP, Dah, Bghi, and Ind increased. The recoveries of Acenl, Acent, Flu, and Phen were highest at 10% of 2-propanol. After that, the recoveries of these PAHs decreased at 15% and 20% of 2-propanol, respectively. For Ant and Flt, the recoveries continuously increased until they were highest at 15% of 2-propanol and the recoveries decreased at 20% of 2-propanol. For Pyr, BaA, Chry, BbF, BkF, BaP, Dah, Bghi, and Ind, the recoveries continuously increased until they were highest at 20% of 2-propanol. Naph could not recover when adding 2-propanol.

The results showed that the solubilities of PAHs increased when adding more 2-propanol as indicated by higher percent recoveries. However, the recoveries of smaller PAHs decreased as the 2-propanol concentration increased because larger PAHs caught the most active sites of disk. Therefore, the smaller PAHs were breakthrough. Naph was earliest breakthrough because it was the smallest PAHs. The 10% of 2-propanol was the optimum concentration for this study by compromising the recoveries of 16 PAHs.

Table 4.6 The results of the effect of the concentration of 2-propanol on the percent recovery of 16 PAHs in 2.00 ppb spiked standard solutions

Compound	2-Propanol concentration (%)									
	0		5		10		15		20	
	Recovery (%)	R.S.D. (%)	Recovery (%)	R.S.D. (%)	Recovery (%)	R.S.D. (%)	Recovery (%)	R.S.D. (%)	Recovery (%)	R.S.D. (%)
Naph	58.66	9.04	-	-	-	-	-	-	-	-
Acenl	49.45	4.11	69.06	2.25	34.93	2.30	8.81	6.05	2.10	8.54
Acent	97.08	3.19	112.15	1.79	95.03	0.54	55.12	2.49	29.80	6.70
Flu	73.38	4.88	107.24	2.67	98.67	1.10	67.73	2.28	32.03	2.73
Phen	87.31	3.07	92.56	0.62	93.50	1.38	88.83	1.83	50.95	5.90
Ant	28.75	6.45	29.85	6.82	30.92	5.66	36.50	6.48	20.84	10.82
Flt	72.44	1.74	81.91	2.42	87.74	2.23	90.21	0.78	84.45	6.70
Pyr	68.96	2.04	76.84	1.40	79.68	2.84	76.35	1.23	79.67	1.61
BaA	54.08	4.13	64.79	6.57	70.00	0.65	74.28	0.20	79.98	1.35
Chry	72.90	2.82	83.69	2.04	102.01	4.57	102.75	0.47	116.86	0.94
BbF	66.16	4.21	74.17	5.02	82.59	1.38	86.03	0.96	96.19	2.04
BkF	56.44	3.73	77.83	11.04	79.76	3.48	92.49	4.37	93.41	1.85
BaP	43.03	3.90	56.27	6.26	56.98	10.28	64.30	2.66	74.91	6.57
Dah	33.57	6.82	44.42	7.91	92.53	4.25	94.72	2.51	99.61	1.45
Bghi	26.95	3.94	48.67	8.13	77.19	5.00	80.10	3.19	86.52	2.09
Ind	42.86	3.54	57.19	5.65	72.69	5.08	75.27	0.58	83.13	0.94

Triplicate analysis

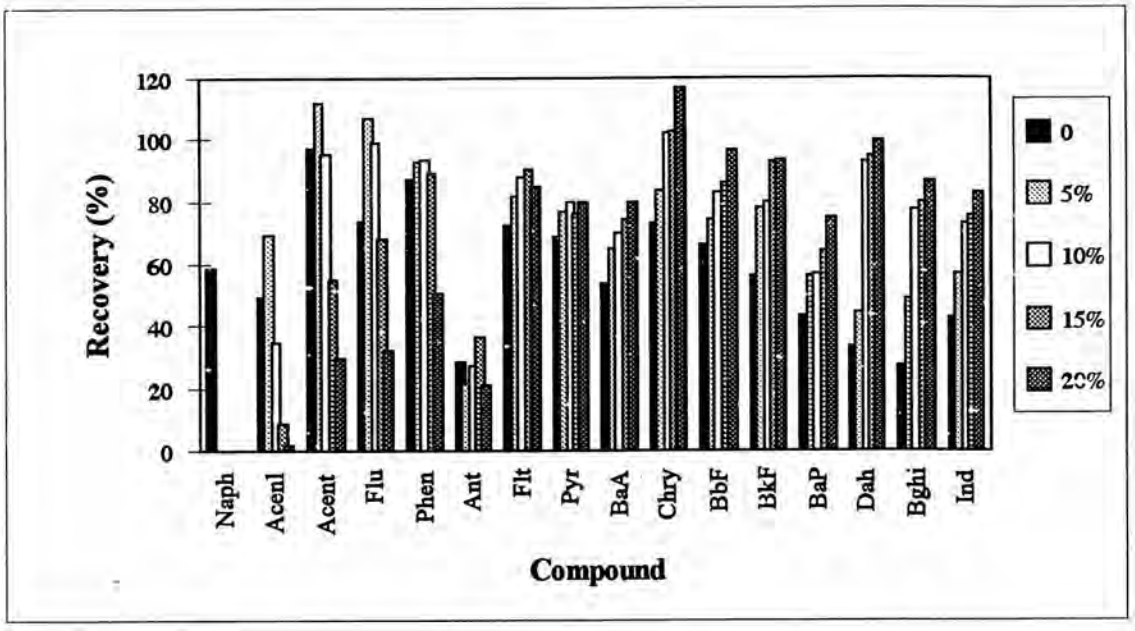

Figure 4.3 The PAHs recoveries at different 2-propanol concentrations in 2.00 ppb spiked standard solutions.

6.2 The Effect of The Concentration of Brij-35

The concentrations of Brij-35 were studied at 0, 0.05, 0.11. 0.30, and 0.50 mM Brij-35 in 2.00 ppb spiked standard solutions. The results of Brij-35 concentrations on the percent recoveries of each PAHs were presented in Table 4.7. The plot of relationship between the percent recoveries and each of PAHs for each of Brij-35 concentrations was shown in Figure 4.4.

The effect of Brij-35 was similar to 2-propanol. When adding 0.05 mM Brij-35, the recoveries of 15 PAHs i.e. Acenl, Acent, Flu, Phen, Ant, Flt, Pyr, BaA, Chry, BbF, BkF, BaP, Dah, Bghi, and Ind increased. The recoveries of Acenl was highest at 0.05 mM Brij-35 and continuously decreased at 0.11, 0.30, and 0.50 mM Brij-35 respectively. Like Acenl, the recoveries of Acent, Dah, Bghi, and Ind were highest at 0.11 mM. After that, the recoveries of these PAHs decreased at 0.11, 0.30, and 0.50 mM Brij-35 respectively. For Flu, the recoveries continuously increased until they were highest at 0.50 mM Brij-35. The recoveries of other PAHs were highest at 0.30 mM Brij-35 and slightly decreased at 0.50 mM Brij-35.

The results showed that the solubilities of PAHs increased when adding more Brij-35 as indicated by higher percent recoveries. However, the recoveries of smaller PAHs decreased as the Brij-35 concentration increased because of the earier breakthrough of smaller PAHs. Because most compounds were highest percent recoveries at 0.30 mM Brij-35, this concentration was the optimum concentration for this study. Although the recoveries of Acent, Dah, Bghi, and Ind decreased at 0.30 mM Brij-35. It was insignificant because the decrease in recoveries were less than 5%.

When 2-propanol was used as organic modifier, the samples were diluted. Moreover, the reducing of toxic solvents and hazardous wastes were the aims of this work. So that, Brij-35 was more suitable to use than 2-propanol. Besides, the recoveries of all PAHs at 0.30 mM Brij-35 were higher than at 10% of 2-propanol. Thus, 0.30 mM Brij-35 was used to increase the solubilities of PAHs in the further experiments.

Table 4.7 The results of the effect of the concentration of Brij-35 on the percent recovery of 16 PAHs in 2.00 ppb spiked standard solutions

Compound	Brij-35 concentration (%)									
	0		0.05		0.11		0.30		0.50	
	Recovery (%)	R.S.D. (%)	Recovery (%)	R.S.D. (%)	Recovery (%)	R.S.D. (%)	Recovery (%)	R.S.D. (%)	Recovery (%)	R.S.D. (%)
Naph	58.66	9.04	-	-	-	-	-	-	-	-
Acenl	49.45	4.11	86.74	1.27	83.79	1.71	78.39	2.62	62.64	3.11
Acent	97.08	3.19	105.69	1.48	110.16	1.18	109.52	1.88	104.37	1.79
Flu	73.38	4.88	99.34	0.96	103.66	3.05	106.53	2.90	107.79	1.82
Phen	87.31	3.07	84.76	0.66	91.19	2.18	98.15	1.08	96.14	2.18
Ant	28.75	6.45	35.77	0.52	39.76	2.28	55.31	4.18	54.13	3.60
Flt	72.44	1.74	75.72	2.52	86.31	1.32	90.78	5.36	87.58	2.89
Pyr	68.96	2.04	68.53	0.43	75.90	1.22	84.15	2.17	79.64	2.77
BaA	54.08	4.13	69.90	1.46	80.60	0.51	84.58	1.11	80.59	3.40
Chry	72.90	2.82	99.06	1.70	110.34	0.94	117.98	1.13	113.94	1.78
BbF	66.16	4.21	82.64	1.67	94.08	1.96	95.32	1.52	90.69	2.91
BkF	56.44	3.73	89.50	4.25	93.68	3.81	103.70	2.66	97.77	1.63
BaP	43.03	3.90	68.82	3.82	81.23	2.01	82.11	0.28	75.97	1.92
Dah	33.57	6.82	75.00	1.76	99.56	2.87	94.74	2.24	68.14	2.46
Bghi	26.95	3.94	75.82	0.74	86.53	1.35	81.59	1.15	57.52	2.07
Ind	42.86	3.54	71.64	1.18	81.68	1.69	79.46	1.67	53.48	4.14

Triplate analysis

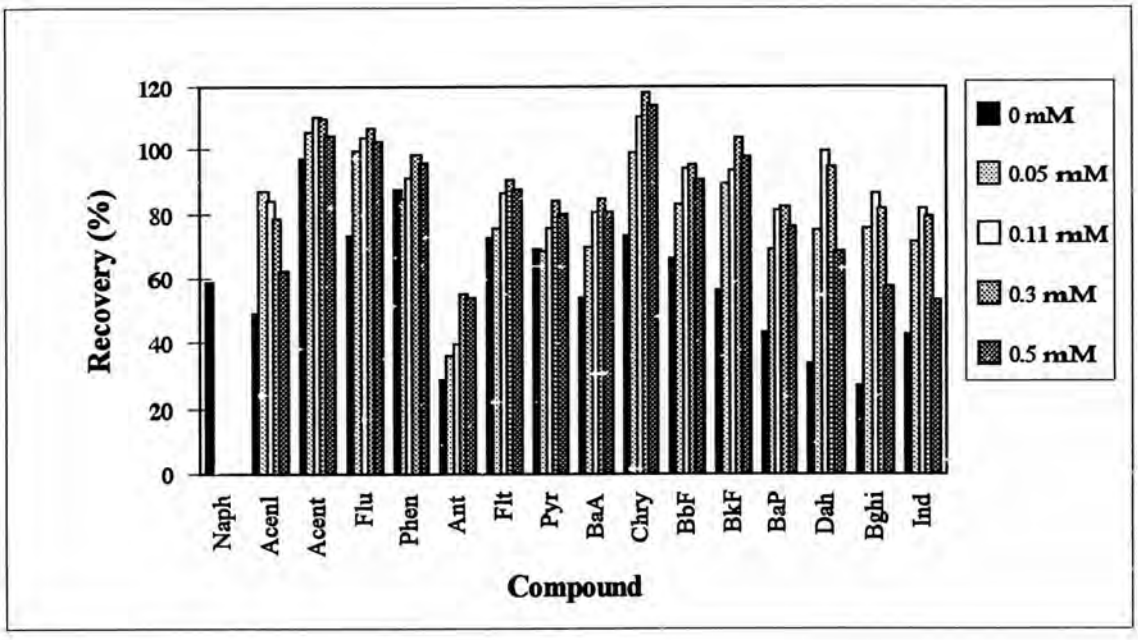

Figure 4.4 The PAHs recoveries at different Brij-35 concentrations in 2.00 ppb spiked standard solutions.

6.3 The Effect of The Volume of Eluting Solvent

In the EPA method 550.1, the eluting solvent was dichloromethane. After elution, dichloromethane was evaporated and acetonitrile was added before detection. In this study, acetonitrile was used as eluting solvent to eliminate the evaporation step. The preliminary study found that the results of dichloromethane and acetonitrile insignificantly differed. The volumes of acetonitrile were studied at 0.50, 0.75, and 1.00 mL. The results of the effect of volume of eluting solvent on the percent recoveries of each PAHs in 2.00 ppb spiked standard solutions containing 0.30 mM Brij-35 were presented in Table 4.8. The plot of relationship between the percent recoveries and each of PAHs for each of volumes of eluting solvent was shown in Figure 4.5.

The results showed that the recoveries of 16 PAHs were not increased when the volume of acetonitrile increased. Thus, 0.50 mL acetonitrile was enough to elute all 16 PAHs. Hence, the volume of acetonitrile at 0.50 mL was chosen as the optimum volume for the small disk extraction method of 16 PAHs.

Table 4.8 The results of the effect of the volume of eluting solvent on the percent recovery of 16 PAHs in 2.00 ppb spiked standard solutions containing 0.30 mM Brij-35

Compound	Volume of eluting solvent (mL)					
	0.50		0.75		1.00	
	Recovery (%)	R.S.D. (%)	Recovery (%)	R.S.D. (%)	Recovery (%)	R.S.D. (%)
Naph	-	-	-	-	-	-
Acenl	78.39	2.62	75.99	2.27	71.96	3.11
Acent	109.52	1.88	105.70	0.61	103.90	6.09
Flu	106.53	2.90	104.17	1.62	101.10	2.67
Phen	98.15	1.08	95.21	1.89	91.16	1.78
Ant	55.31	4.18	52.58	2.36	49.66	2.12
Flt	90.78	5.36	86.64	4.75	85.79	4.26
Pyr	84.15	2.17	83.51	1.04	81.95	2.14
BaA	84.58	1.11	80.45	1.15	76.62	1.93
Chry	117.98	1.13	114.79	3.43	110.75	1.67
BbF	95.32	1.52	98.21	1.00	97.63	3.79
BkF	103.70	2.66	101.82	2.82	98.57	4.99
BaP	82.11	0.28	80.43	4.28	78.53	1.93
Dah	94.74	2.24	90.43	5.51	88.42	2.50
Bghi	81.59	1.15	79.76	3.53	77.35	5.81
Ind	79.46	1.67	77.61	7.65	75.30	7.83

Triplicate analysis

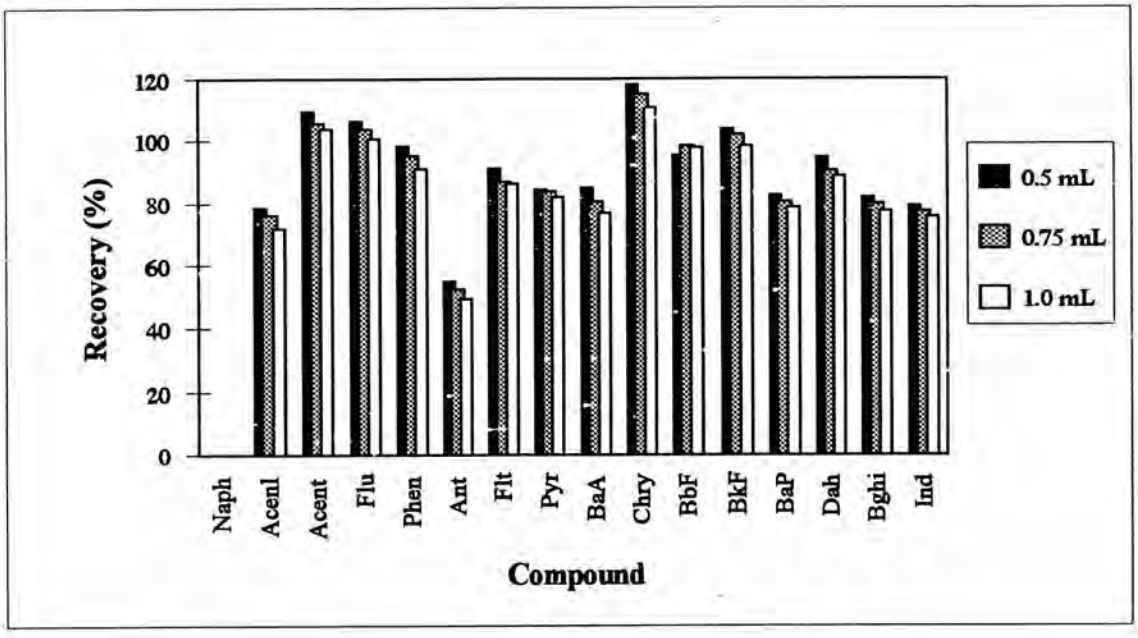

Figure 4.5 The PAHs recoveries of 2.00 ppb spiked standard solutions containing 0.30 mM Brij-35 at different volumes of eluting solvent (acetonitrile).

6.4 The Effect of The Elution Time

The time required for the elution of PAHs from disk was studied at 5, 15, 30, 45, and 60 min. The results of the effect of elution time on the percent recoveries of each PAHs in 2.00 ppb spiked standard solutions containing 0.30 mM Brij-35 were presented in Table 4.9. The plot of relationship between the percent recoveries and each of PAHs for each of elution times was shown in Figure 4.6.

The results showed that the recoveries of smaller PAHs (i.e. Acenl, Flu, Phen, Flt, Pyr, and Chry) were highest at 5 min of elution time. While the recoveries of larger PAHs (i.e. BbF, BkF, and Dah) were highest at 15 min of elution time. Moreover, the recoveries of all PAHs insignificantly changed after 15 min. So that the minimum time for elution of all PAHs was 15 min.

Table 4.9 The results of the effect of the elution time on the percent recovery of 16 PAHs in 2.00 ppb spiked standard solutions containing 0.30 mM Brij-35

Compound	Elution time (min)									
	5		15		30		45		60	
	Recovery (%)	R.S.D. (%)	Recovery (%)	R.S.D. (%)	Recovery (%)	R.S.D. (%)	Recovery (%)	R.S.D. (%)	Recovery (%)	R.S.D. (%)
Naph	-	-	-	-	-	-	-	-	-	-
Acenl	79.62	4.43	77.96	9.26	78.39	2.62	72.54	2.08	73.80	3.38
Acent	109.44	5.21	107.58	6.53	109.52	1.88	105.09	1.40	105.22	2.44
Flu	108.87	4.50	105.29	4.32	106.53	2.90	105.78	3.25	101.50	2.10
Phen	98.82	1.09	95.59	0.66	98.15	1.08	95.51	3.01	93.20	1.88
Ant	34.60	4.52	50.69	2.32	55.31	4.18	49.93	4.00	48.48	2.35
Flt	92.66	7.27	89.59	1.34	90.78	5.36	88.69	8.02	91.70	2.06
Pyr	84.55	1.68	80.94	1.08	84.15	2.17	81.94	1.44	80.27	1.11
BaA	82.72	1.75	80.75	1.54	84.58	1.11	82.85	1.60	80.49	1.21
Chry	118.85	1.69	114.61	0.83	117.98	1.13	117.13	1.66	113.67	1.27
BbF	95.68	0.99	99.59	3.25	95.32	1.52	98.72	2.00	97.64	2.28
BkF	100.59	4.53	105.97	6.84	103.70	2.66	97.19	1.58	100.56	2.28
BaP	80.38	1.41	77.28	2.92	82.11	0.28	77.64	1.57	75.88	1.71
Dah	89.66	8.34	97.29	1.54	94.74	2.24	95.68	1.41	91.65	1.12
Bghi	74.61	7.47	81.46	0.65	81.59	1.15	83.54	2.38	78.78	3.92
Ind	57.75	4.53	79.16	1.88	79.46	1.67	78.11	2.15	75.63	3.72

Triplate analysis

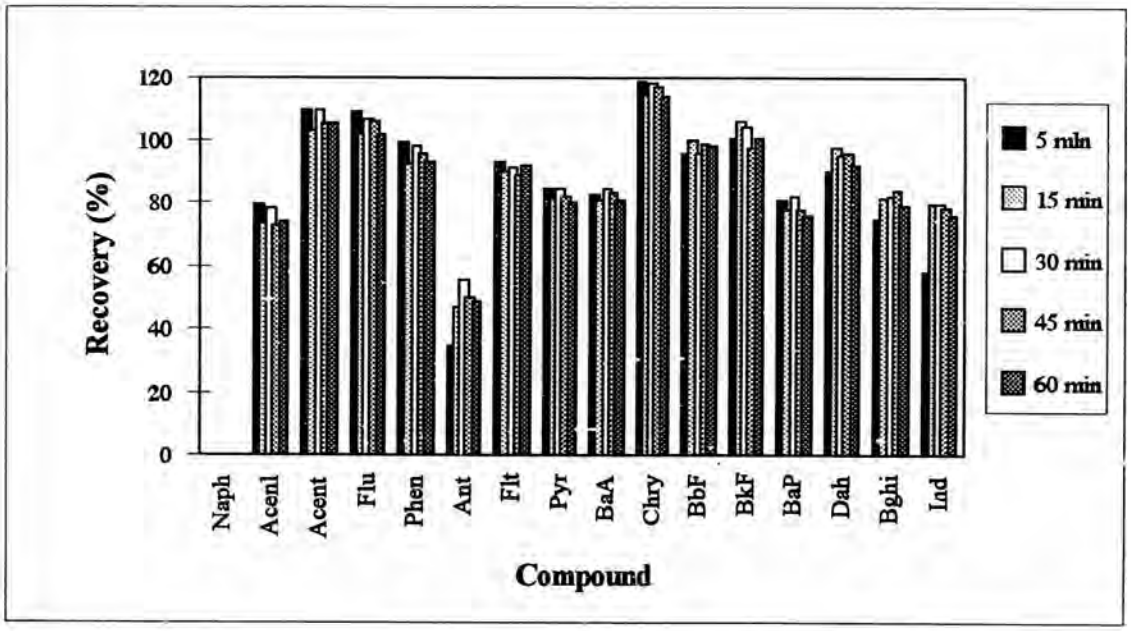

Figure 4.6 The PAHs recoveries of 2.00 ppb spiked standard solutions containing 0.30 mM Brij-35 at different elution times.

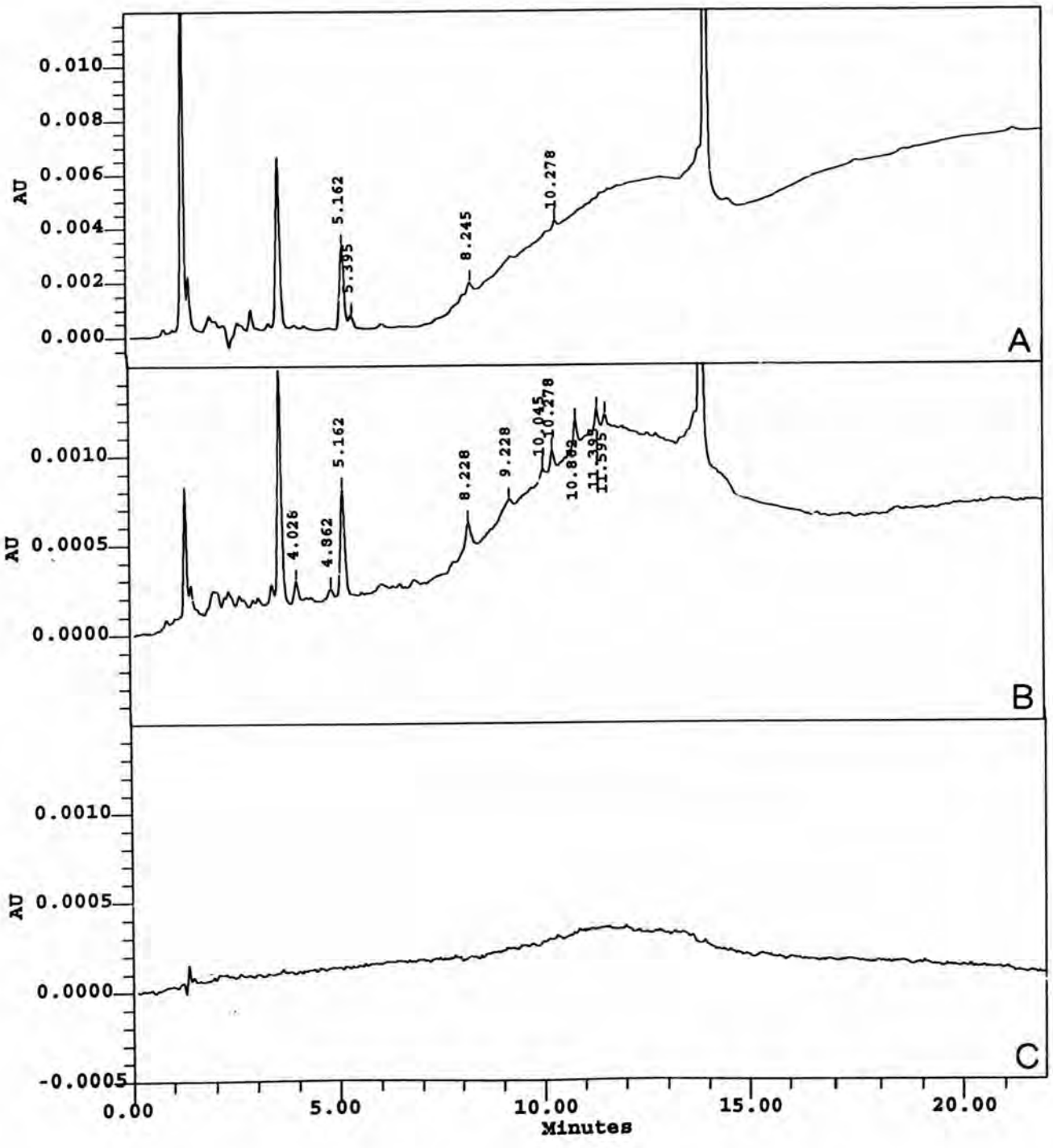

Figure 4.8 The chromatogram of SPM drinking water [Polypropylene bottle] (sample 1) concentrated 200-fold on a small C_{18} disk by the HPLC conditions in Table 4.1.

A At 230 nm

B At 270 nm

C At 350 nm

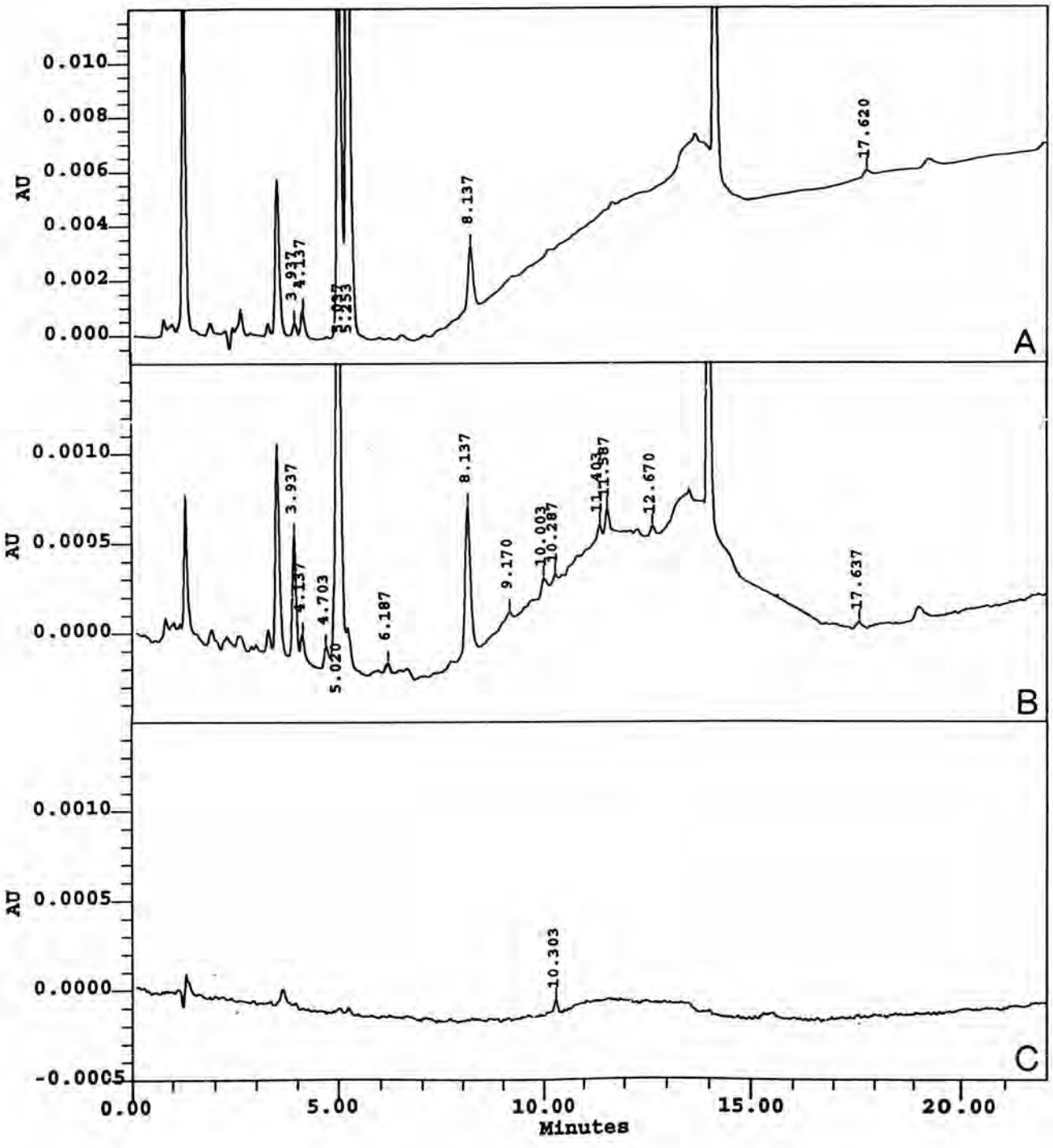

Figure 4.9 The chromatogram of fresh drinking water [Polypropylene bottle] (sample 2) concentrated 200-fold on a small C_{18} disk by the HPLC conditions in Table 4.1.

A At 230 nm

B At 270 nm

C At 350 nm

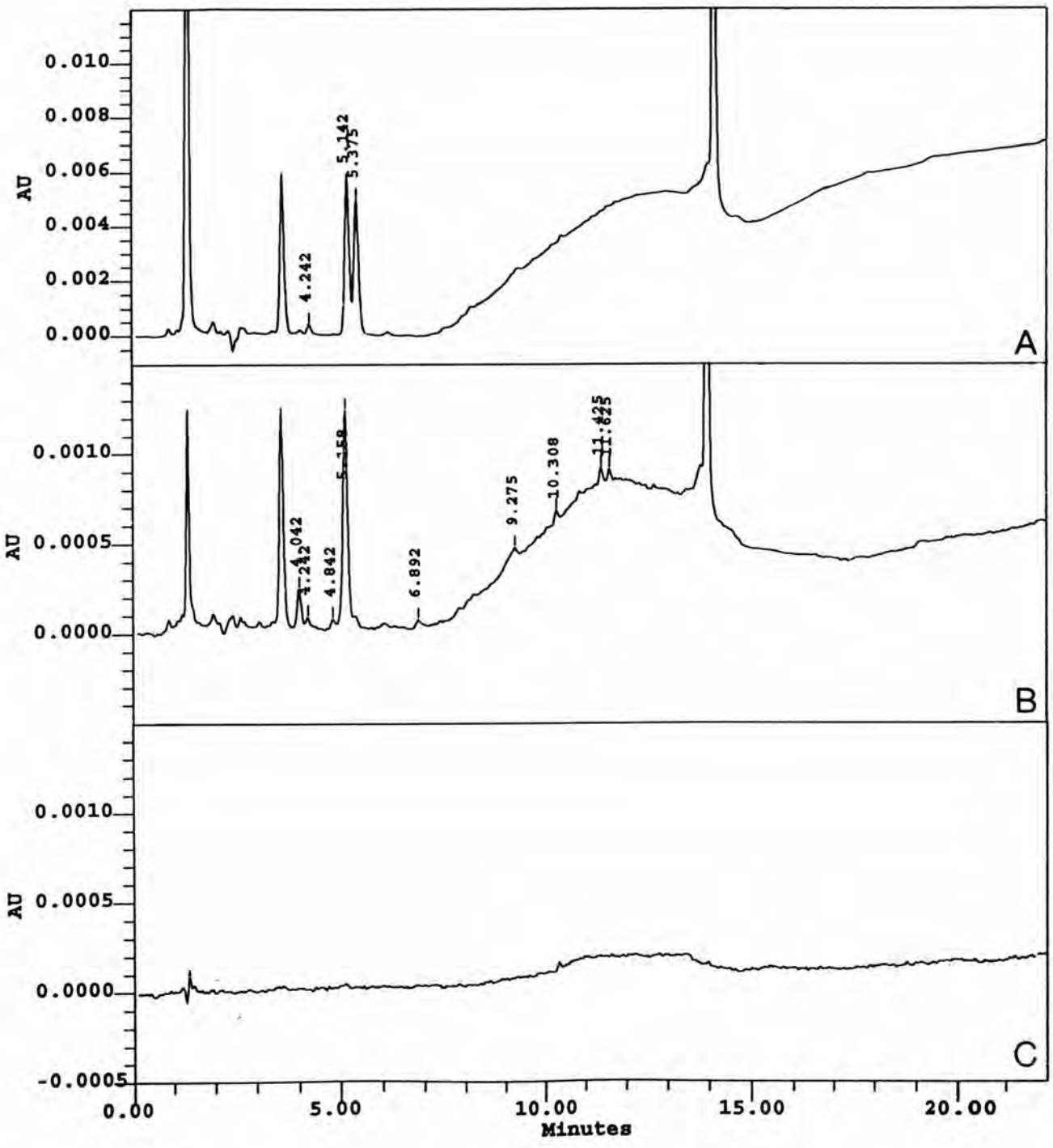

Figure 4.10 The chromatogram of puntip drinking water [Polypropylene bottle] (sample 3) concentrated 200-fold on a small C_{18} disk by the HPLC conditions in Table 4.1.

A At 230 nm

B At 270 nm

C At 350 nm

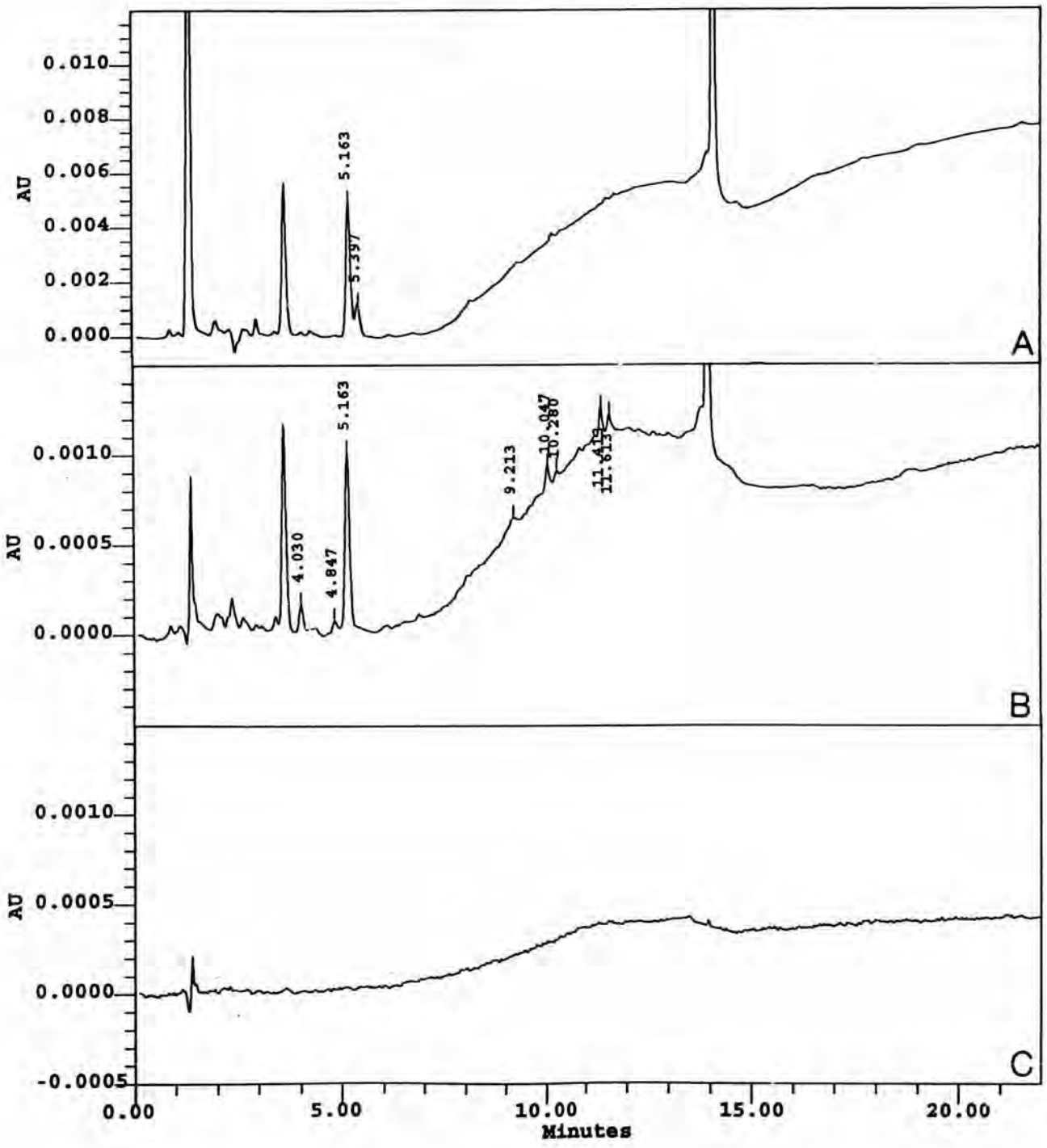

Figure 4.11 The chromatogram of crystal drinking water [Polypropylene bottle] (sample 4) concentrated 200-fold on a small C_{18} disk by the HPLC conditions in Table 4.1.

A At 230 nm

B At 270 nm

C At 350 nm

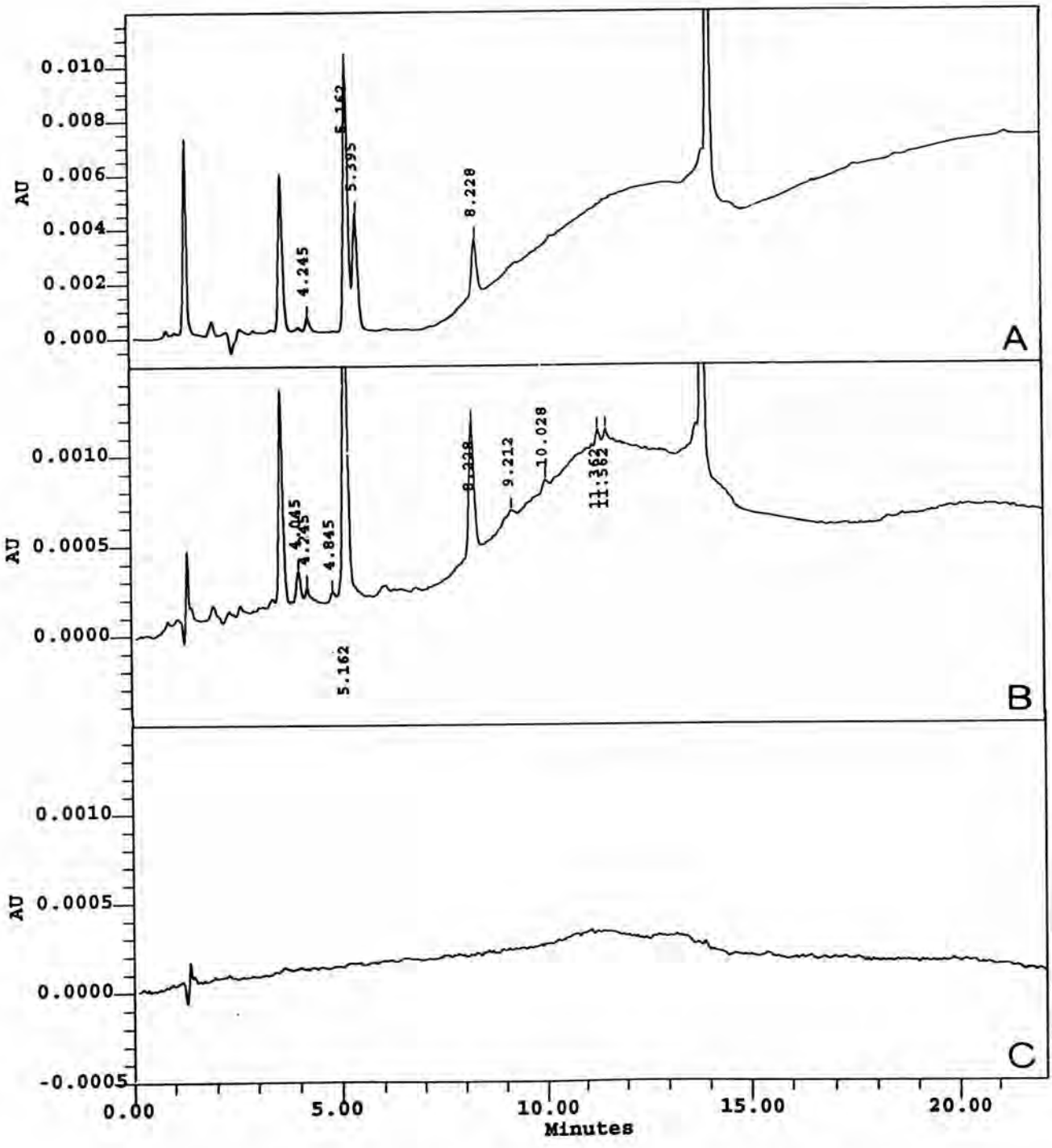

Figure 4.12 The chromatogram of sprinkle drinking water [Polypropylene bottle] (sample 5) concentrated 200-fold on a small C_{18} disk by the HPLC conditions in Table 4.1.

A At 230 nm

B At 270 nm

C At 350 nm

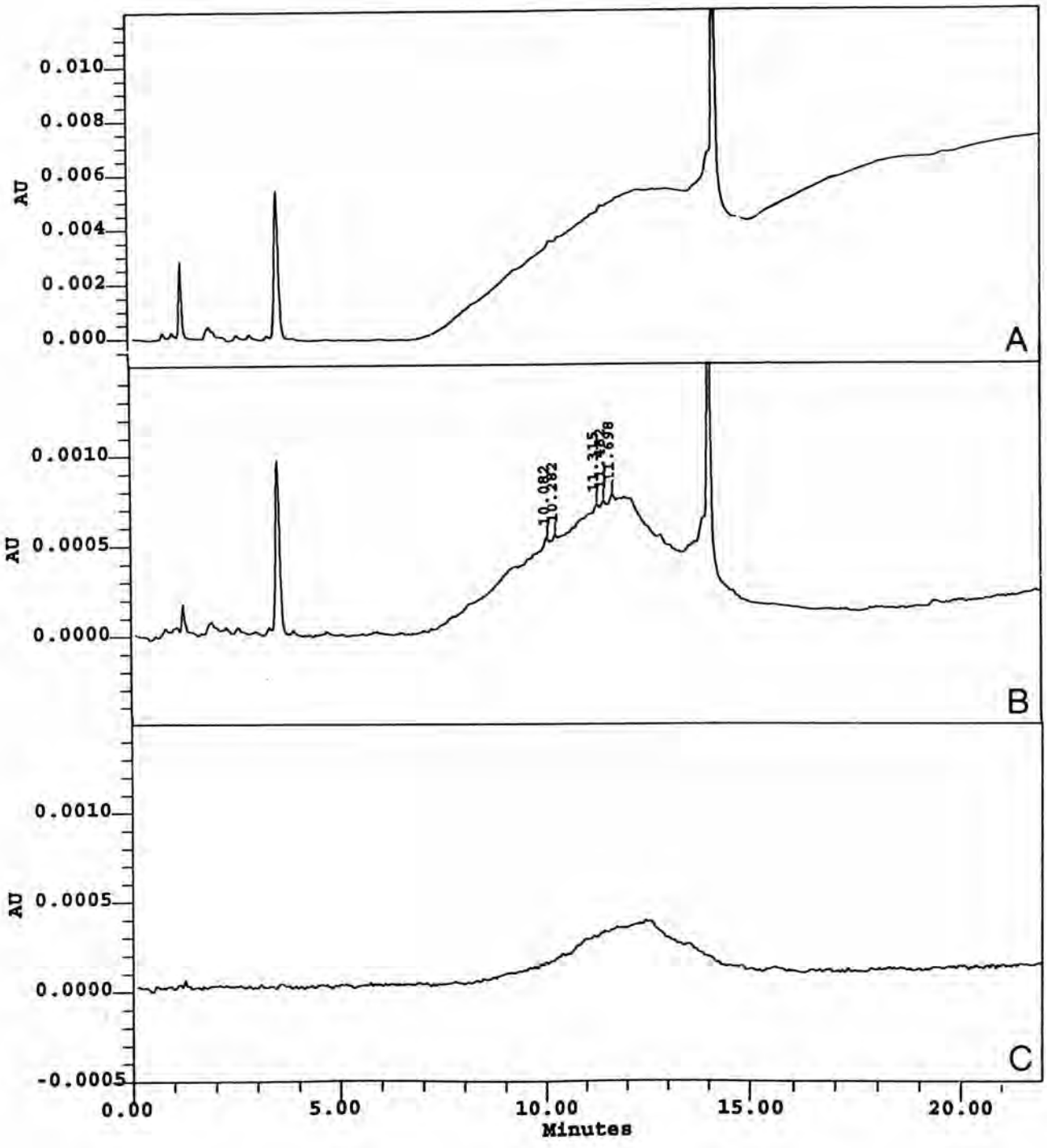

Figure 4.13 The chromatogram of idea drinking water [Polypropylene bottle] (sample 6) concentrated 200-fold on a small C_{18} disk by the HPLC conditions in Table 4.1.

A At 230 nm

B At 270 nm

C At 350 nm

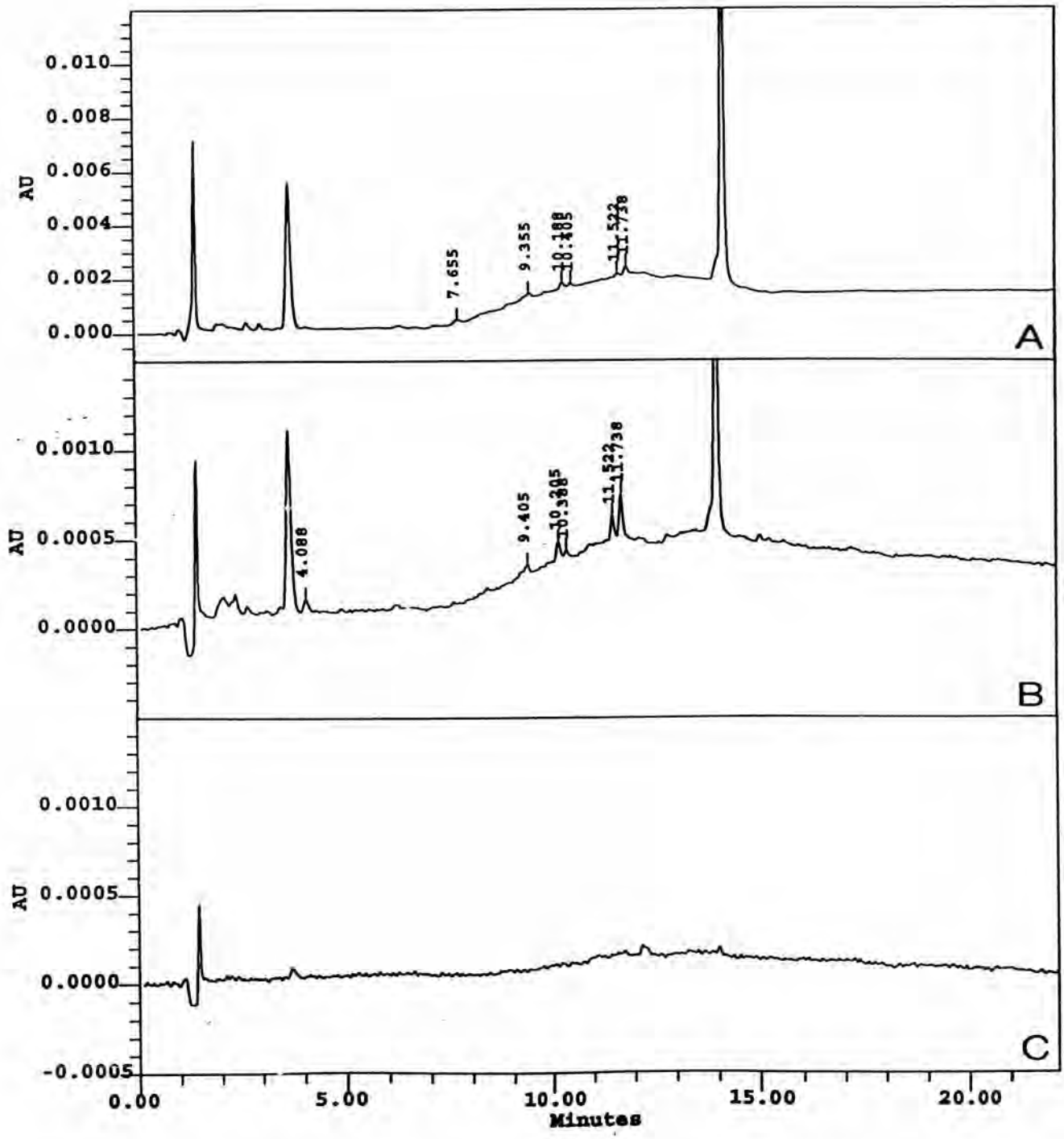

Figure 4.14 The chromatogram of crystal drinking water [Poly(ethylene terephthalate) bottle] (sample 7) concentrated 200-fold on a small C_{18} disk by the HPLC conditions in Table 4.1.

A At 230 nm

B At 270 nm

C At 350 nm

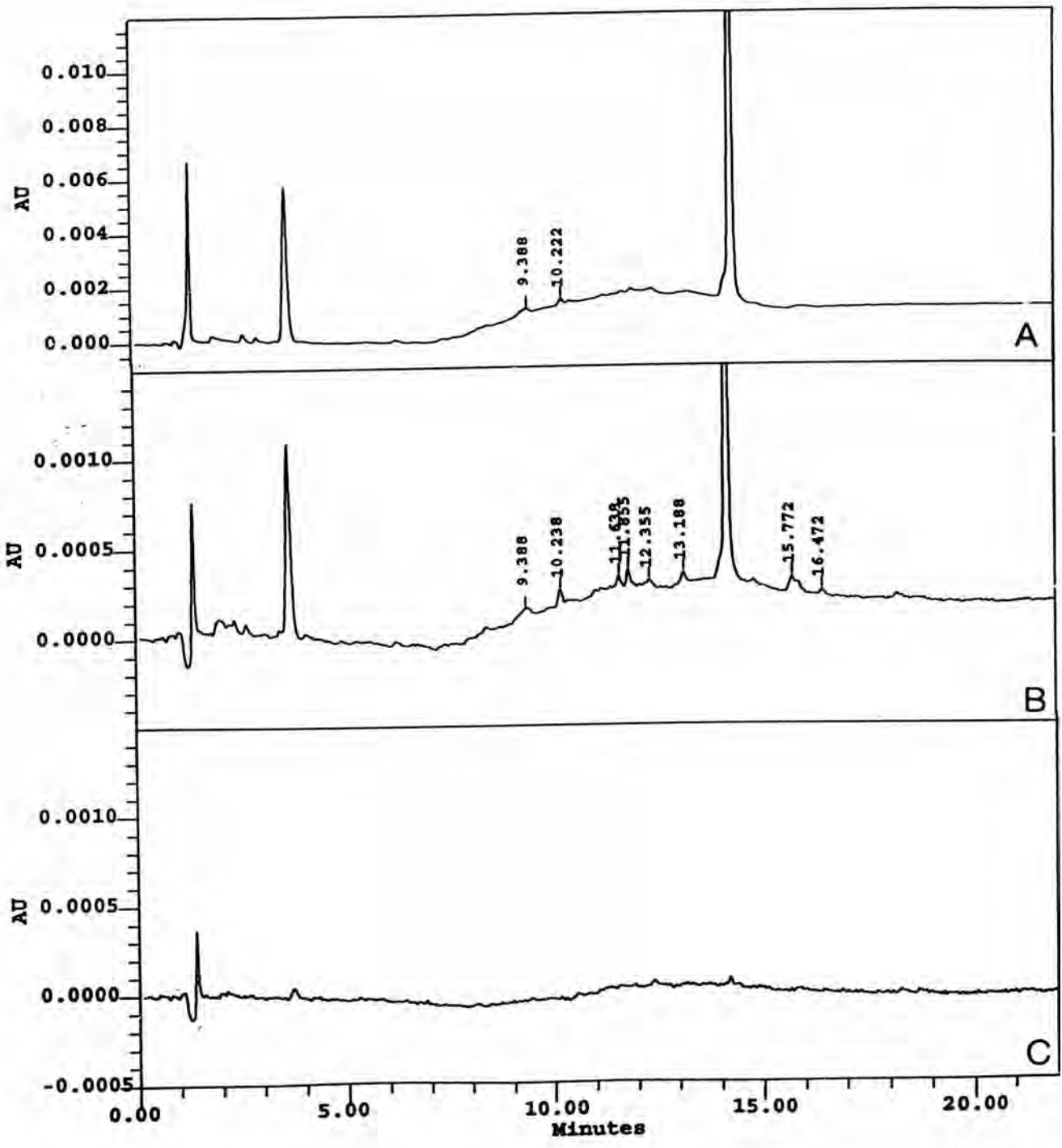

Figure 4.15 The chromatogram of sprinkle drinking water [Poly(ethylene terephthalate) bottle] (sample 8) concentrated 200-fold on a small C_{18} disk by the HPLC conditions in Table 4.1.

A At 230 nm

B At 270 nm

C At 350 nm

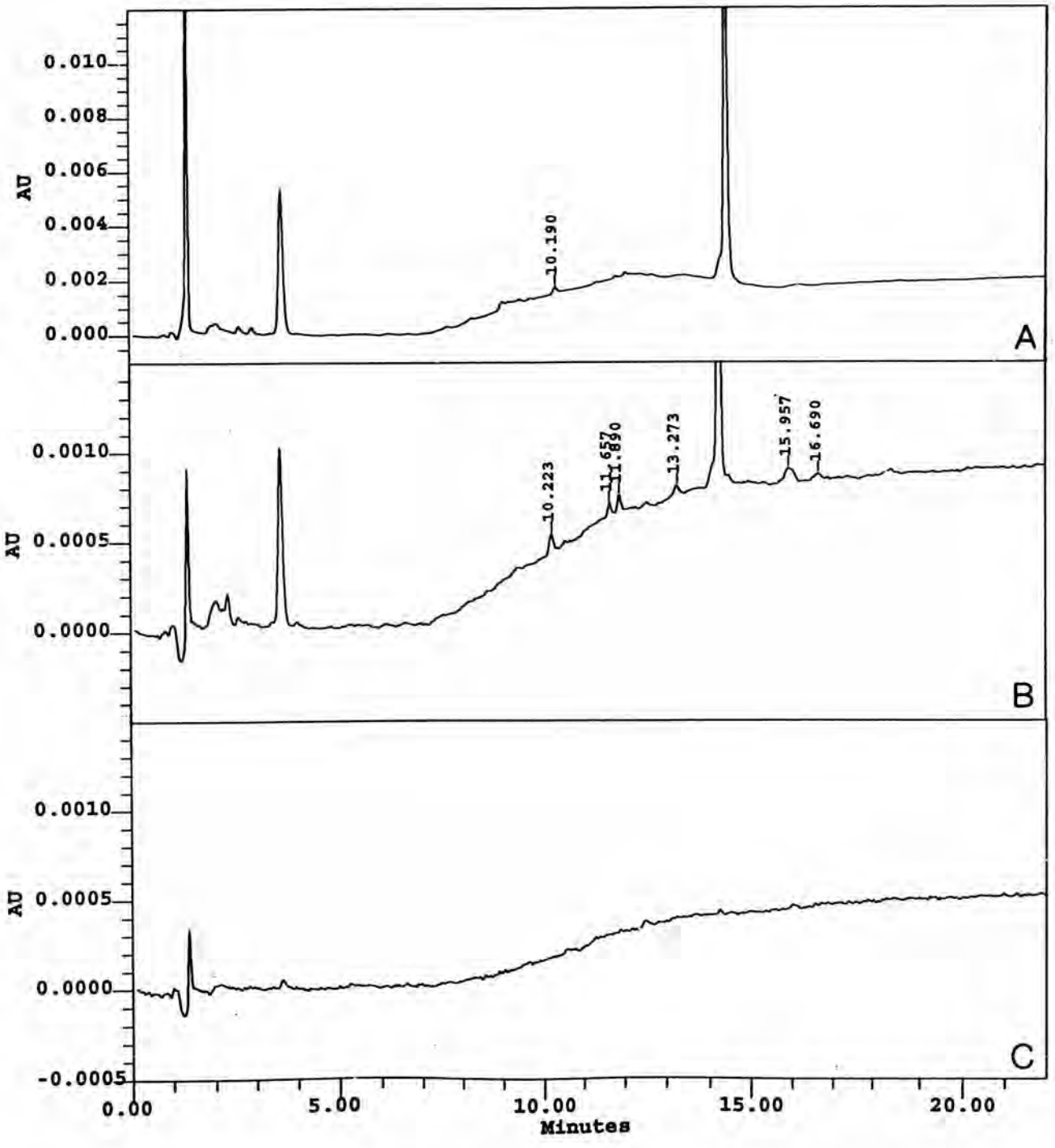

Figure 4.16 The chromatogram of singha drinking water [Poly(ethylene terephthalate) bottle] (sample 9) concentrated 200-fold on a small C_{18} disk by the HPLC conditions in Table 4.1.

A At 230 nm

B At 270 nm

C At 350 nm

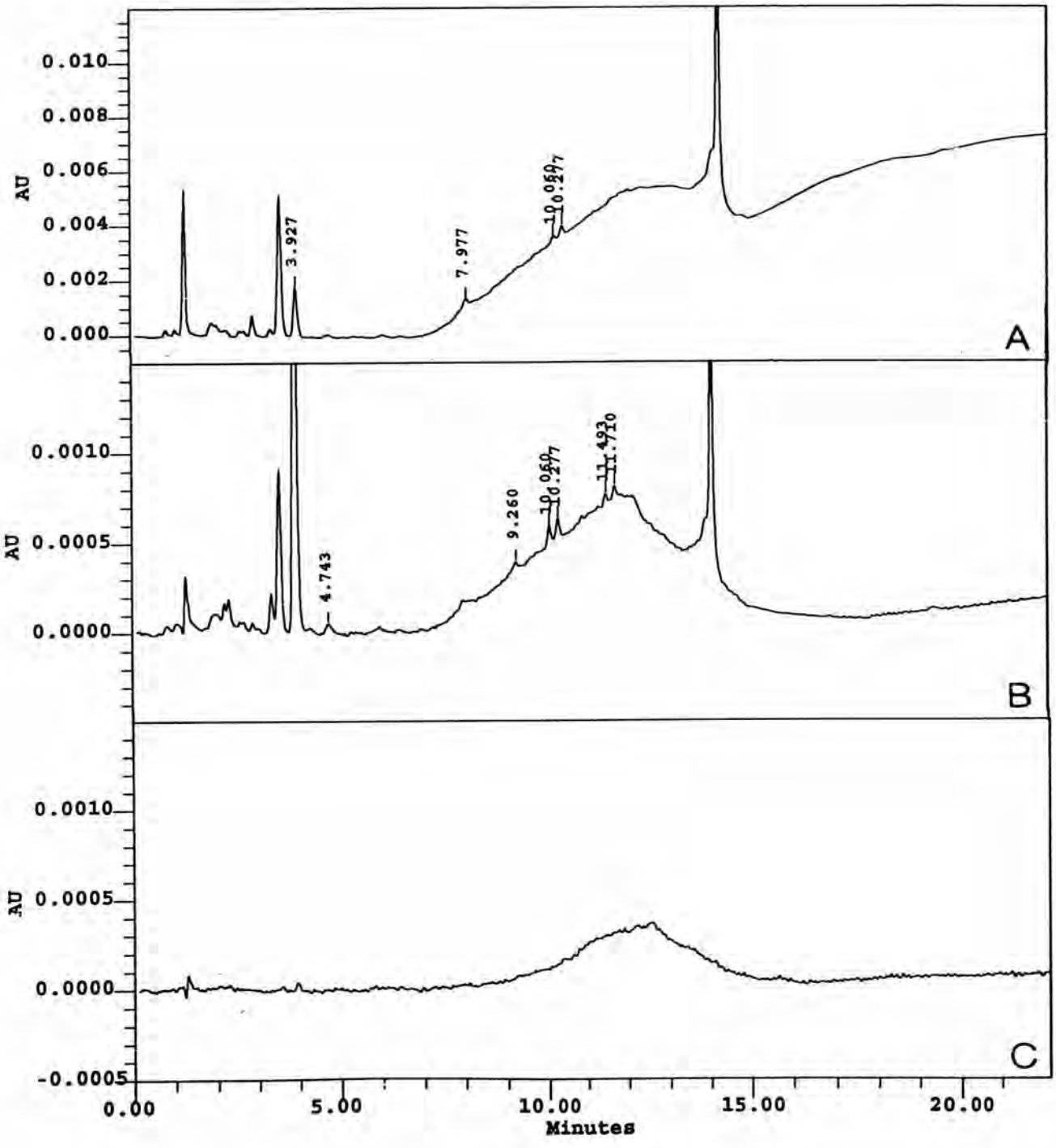

Figure 4.17 The chromatogram of volvic natural mineral water (sample 10) concentrated 200-fold on a small C_{18} disk by the HPLC conditions in Table 4.1.

A At 230 nm

B At 270 nm

C At 350 nm

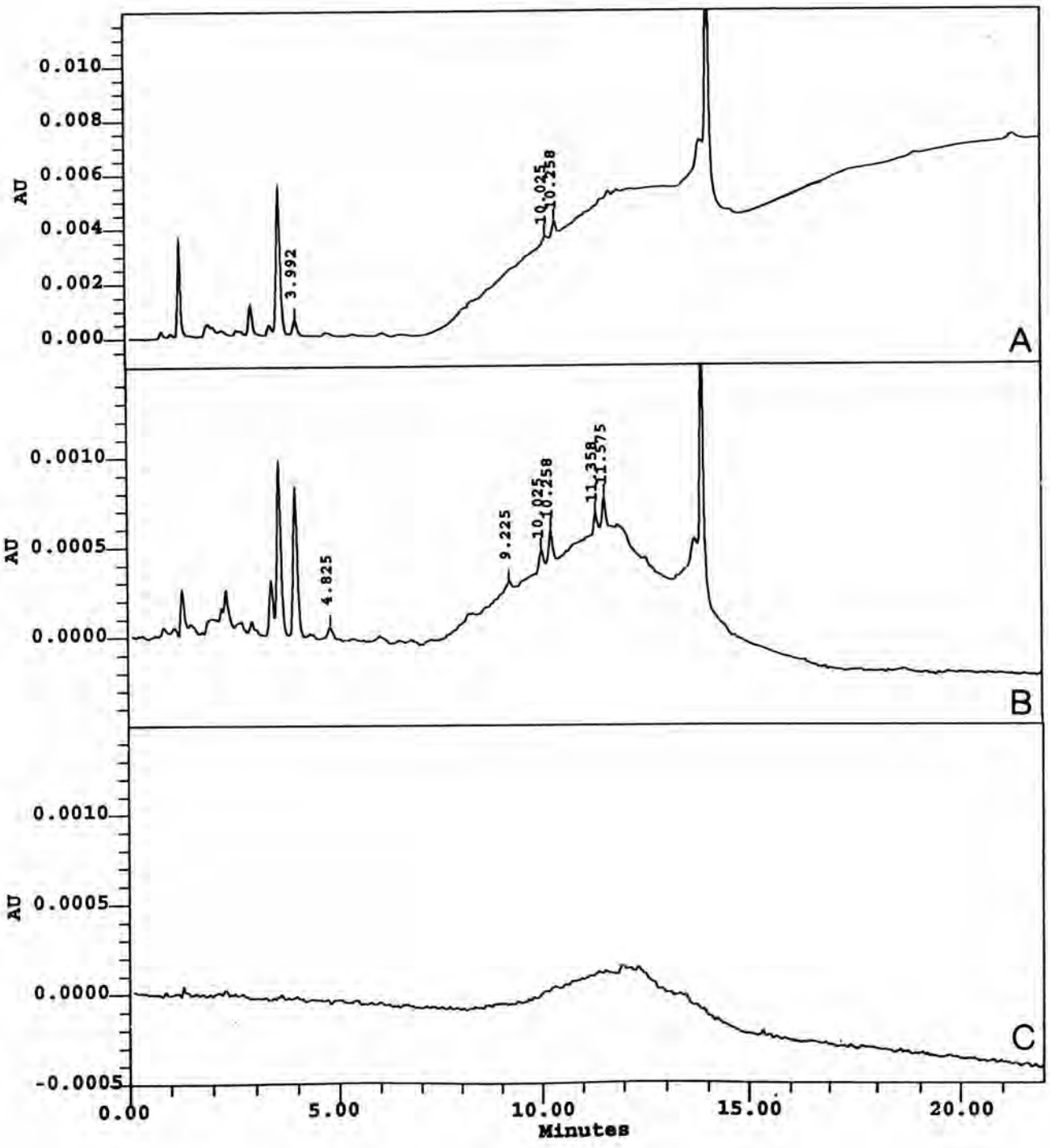

Figure 4.18 The chromatogram of vittel natural mineral water (sample 11) concentrated 200-fold on a small C_{18} disk by the HPLC conditions in Table 4.1.

A At 230 nm

B At 270 nm

C At 350 nm

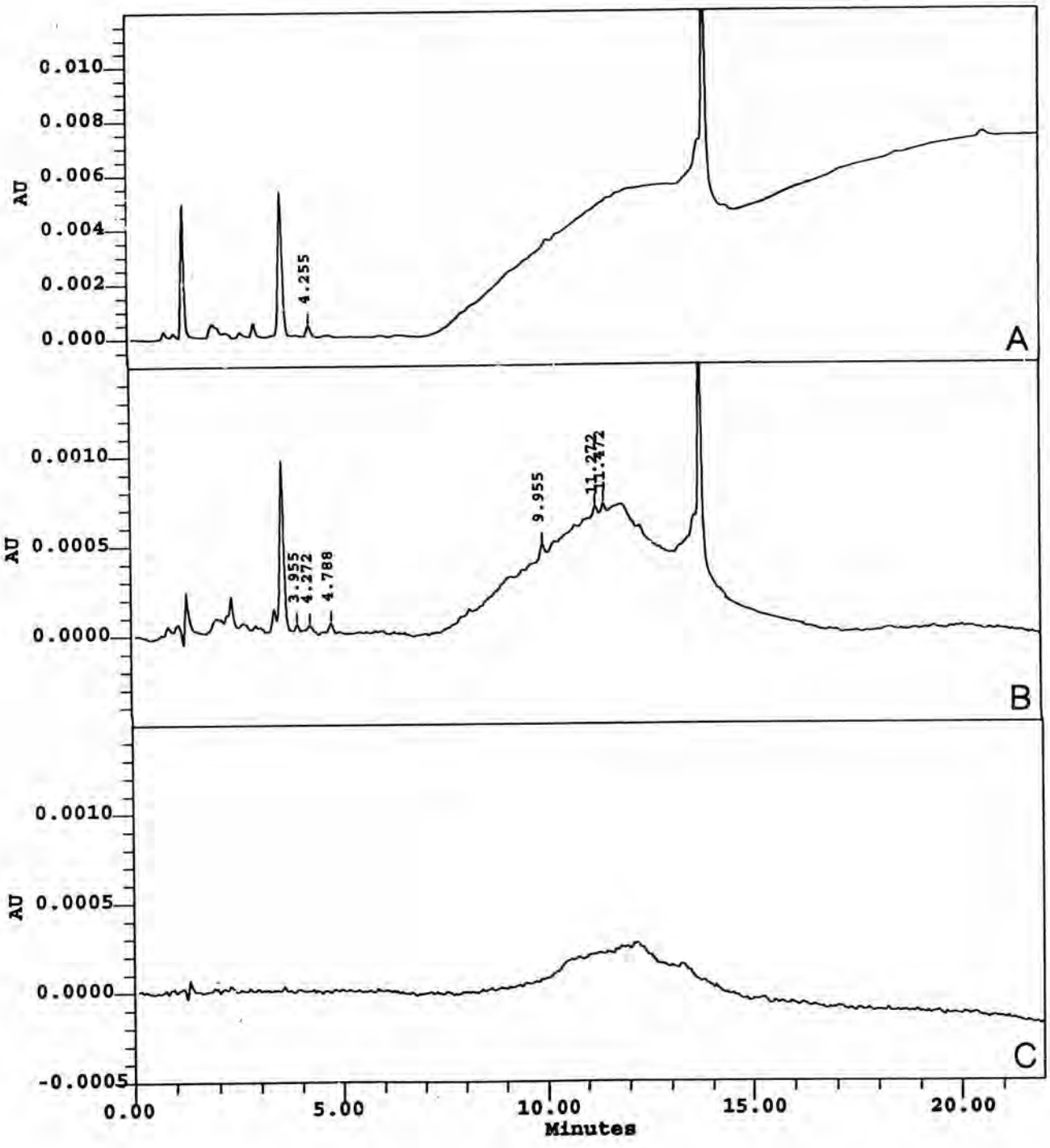

Figure 4.19 The chromatogram of aura natural mineral water (sample 12) concentrated 200-fold on a small C_{18} disk by the HPLC conditions in Table 4.1.

A At 230 nm

B At 270 nm

C At 350 nm

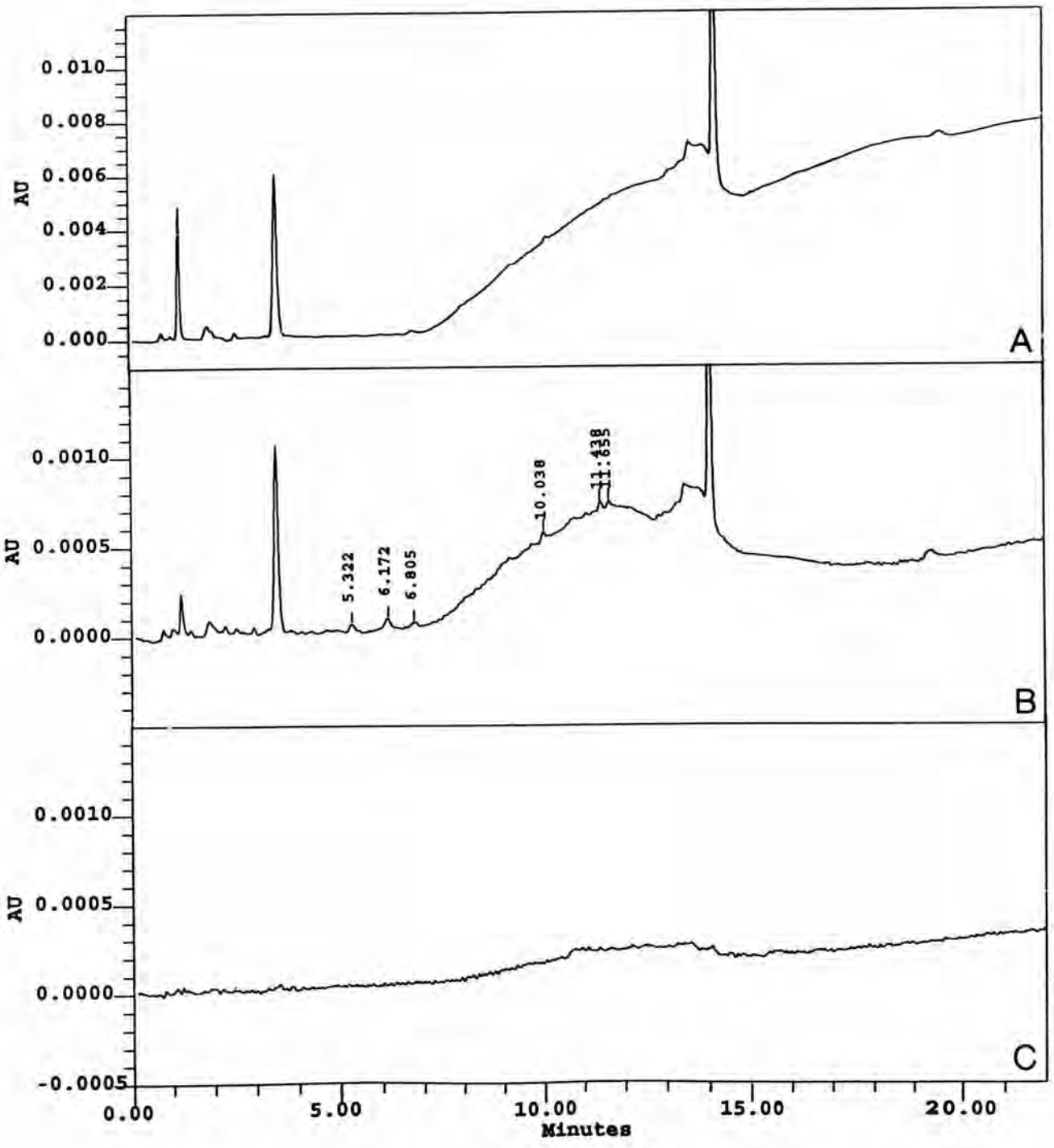

Figure 4.20 The chromatogram of ice (sample 13) concentrated 200-fold on a small C_{18} disk by the HPLC conditions in Table 4.1.

A At 230 nm

B At 270 nm

C At 350 nm

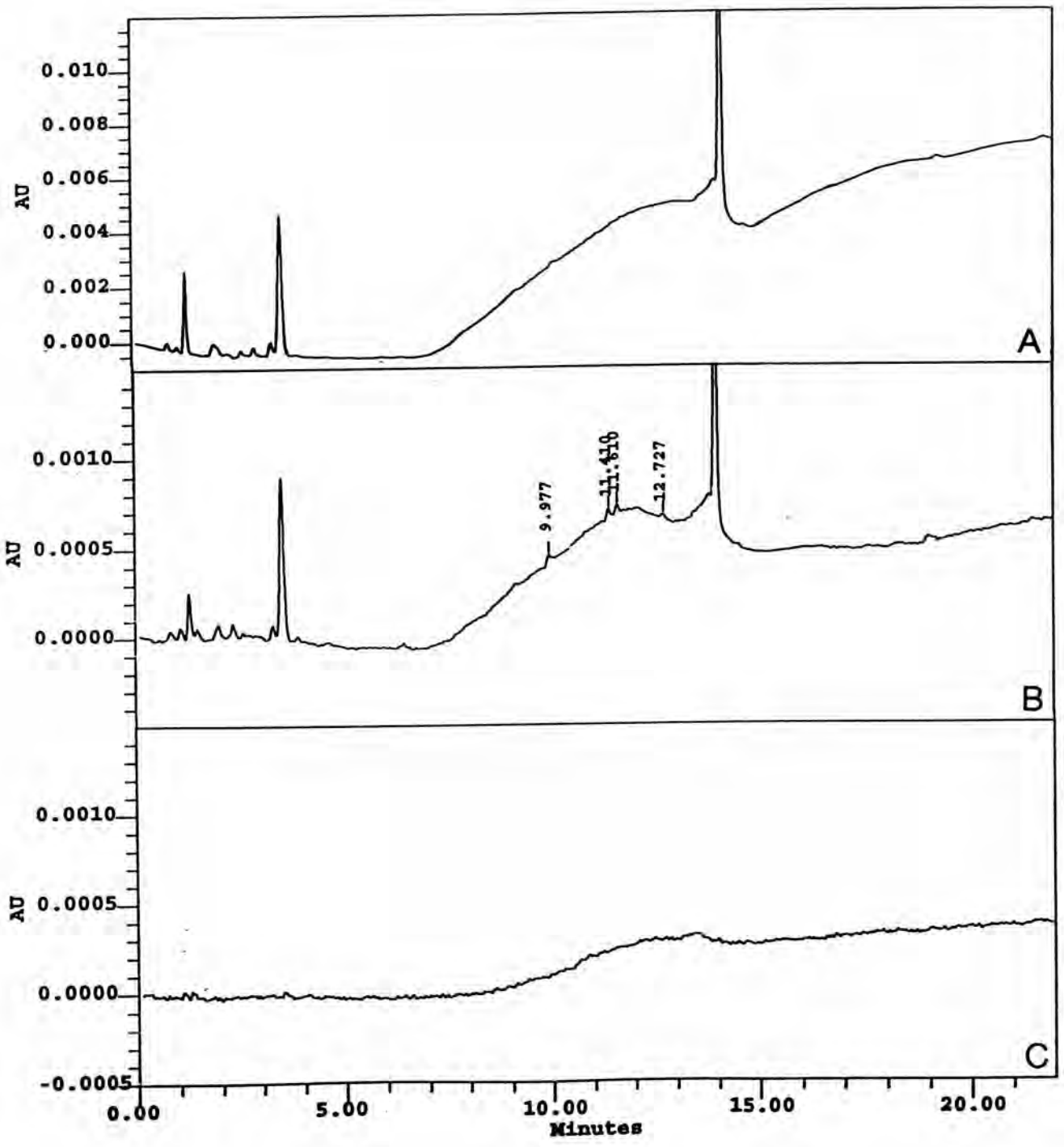

Figure 4.21 The chromatogram of tap water (sample 14) concentrated 200-fold on a small C_{18} disk by the HPLC conditions in Table 4.1.

A At 230 nm

B At 270 nm

C At 350 nm

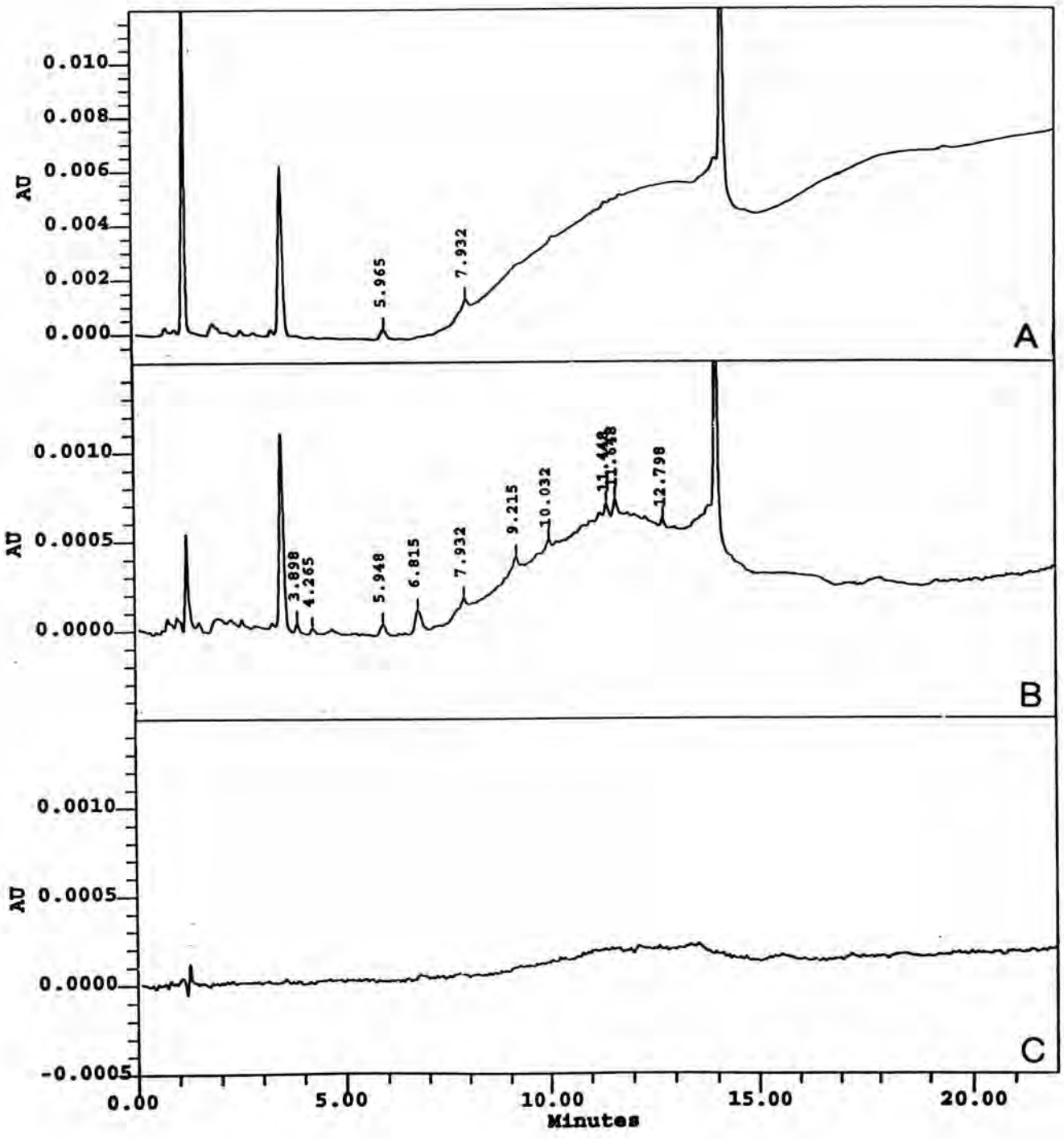

Figure 4.22 The chromatogram of pool water (sample 15) concentrated 200-fold on a small C_{18} disk by the HPLC conditions in Table 4.1.

A At 230 nm

B At 270 nm

C At 350 nm